

1 **Supplemental Information**

2

3 **Mechanism of the hydroxy radical oxidation of methacryloyl peroxyxynitrate (MPAN) and its**  
4 **pathway toward secondary organic aerosol formation in the atmosphere**

5

6 Tran B. Nguyen,<sup>1\*</sup> Kelvin H. Bates,<sup>2</sup> John D. Crouse,<sup>1</sup> Rebecca H. Schwantes,<sup>1</sup> Xuan Zhang,<sup>1</sup>  
7 Henrik G. Kjaergaard,<sup>3</sup> Jason D. Surratt,<sup>4</sup> Peng Lin,<sup>5</sup> Alexander Laskin,<sup>5</sup> John H. Seinfeld,<sup>2,6</sup> and  
8 Paul O. Wennberg<sup>1,6</sup>

9

10 1. Division of Geological and Planetary Sciences, California Institute of Technology, Pasadena,  
11 California, USA

12 2. Division of Chemistry and Chemical Engineering, California Institute of Technology,  
13 Pasadena, California, USA

14 3. Department of Chemistry, University of Copenhagen, Copenhagen, Denmark

15 4. Department of Environmental Sciences and Engineering, University of North Carolina at  
16 Chapel Hill, Chapel Hill, North Carolina, USA

17 5. W.R. Wiley Environmental Molecular Science Laboratory, Pacific Northwest National  
18 Laboratory, Richland, Washington, USA

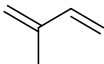
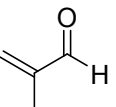
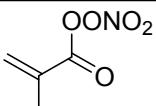
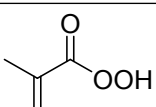
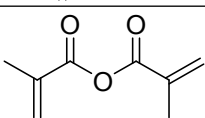
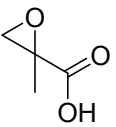
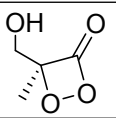
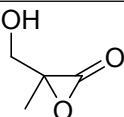
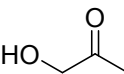
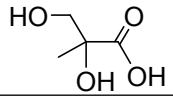
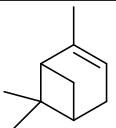
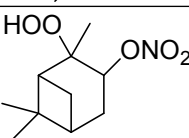
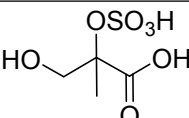
19 6. Division of Engineering and Applied Science, California Institute of Technology, Pasadena,  
20 California, USA

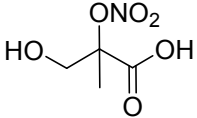
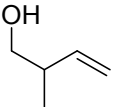
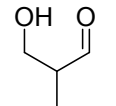
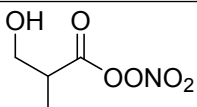
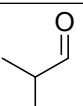
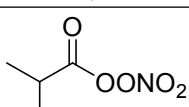
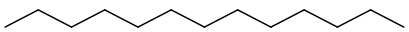
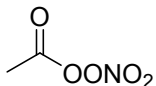
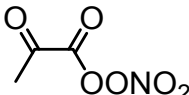
21

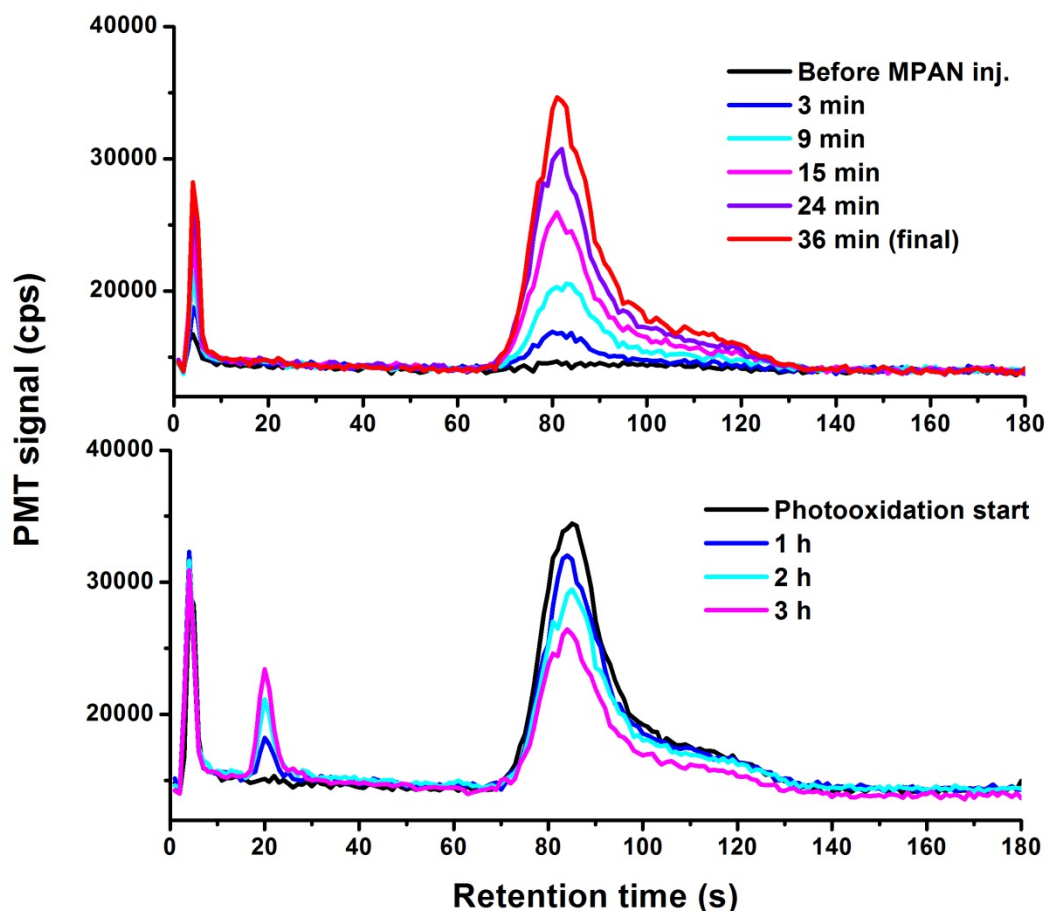
22 *\*author to whom correspondence should be directed: [tbn@caltech.edu](mailto:tbn@caltech.edu)*

23

1 **Table S1:** Chemical structure and names for the organic compounds discussed in this work.

Chemical structure	Name used in paper	IUPAC name (generated from Chemdraw, Cambridgesoft)
	isoprene	isoprene
	methacrolein (MACR)	methacrylaldehyde
	methacryloyl peroxy nitrate (MPAN)	methacrylic nitric peroxyanhydride
	methacrylic peroxy acid (MPAA)	2-methylprop-2-eneperoxy acid
	methacrylic anhydride	methacrylic anhydride
	methacrylic acid epoxide (MAE)	2-methyloxirane-2-carboxylic acid
	dioxoketone (DOK)	(S)-4-(hydroxymethyl)-4-methyl-1,2-dioxetan-3-one
	hydroxymethyl methyl- $\alpha$ -lactone (HMML)	3-(hydroxymethyl)-3-methyloxiran-2-one
	hydroxyacetone (HAC)	1-hydroxypropan-2-one
	2-methylglyceric acid (2MGA)	2,3-dihydroxy-2-methylpropanoic acid
	$\alpha$ -pinene ( $\alpha$ -PIN)	2,6,6-trimethylbicyclo[3.1.1]hept-2-ene
	pinene nitrooxyhydroperoxide (PNP)	2-hydroperoxy-2,6,6-trimethylbicyclo[3.1.1]heptan-3-yl nitrate
	sulfate ester of 2-methylglyceric acid (2MGA-sulfate)	3-hydroxy-2-methyl-2-(sulfooxy)propanoic acid

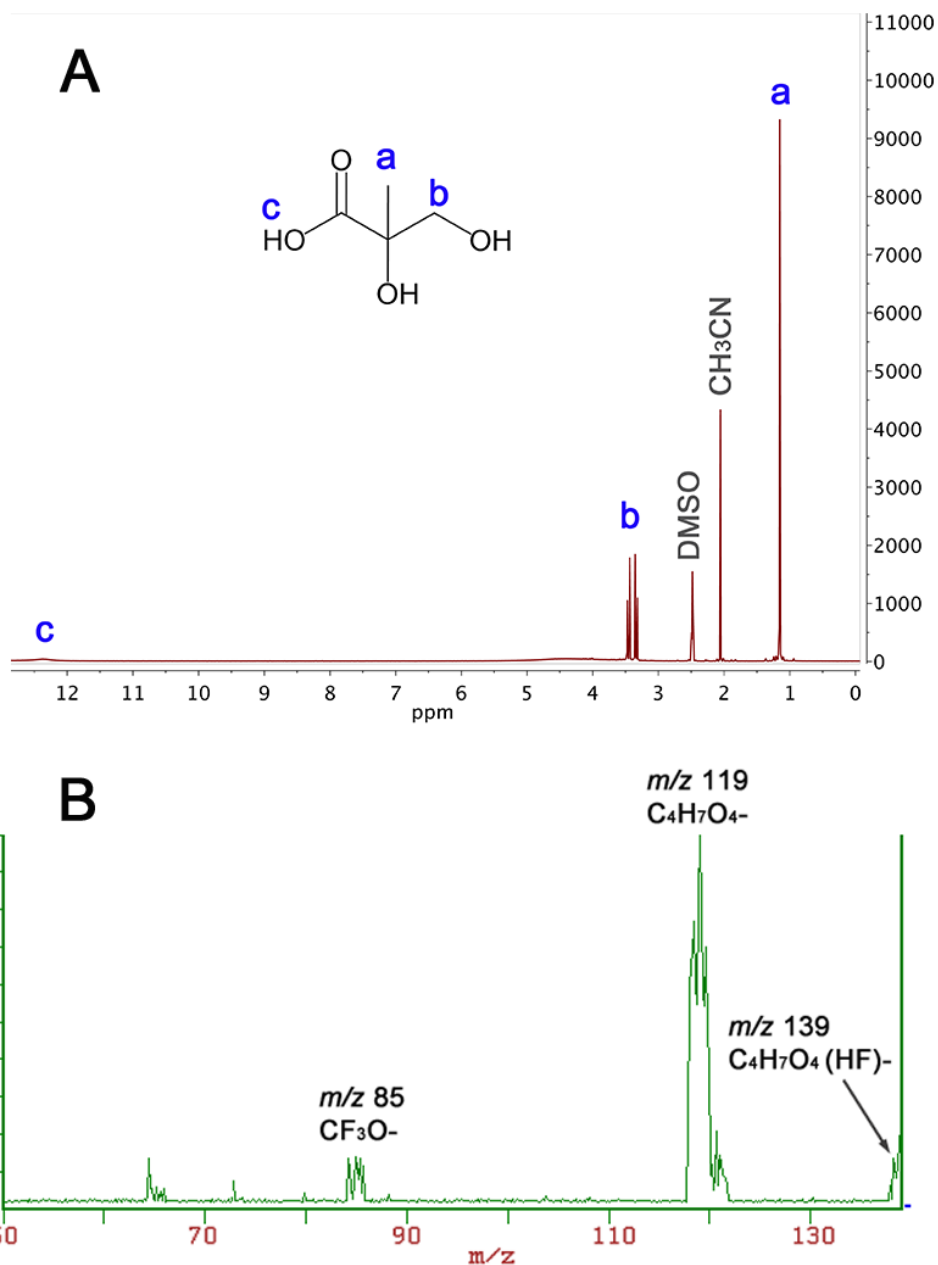
	nitrate ester of 2-methylglyceric acid (2MGA-nitrate)	3-hydroxy-2-methyl-2-(nitrooxy)propanoic acid
	2-methyl-but-3-ene-1-ol (231MBO)	2-methyl-but-3-ene-1-ol
	hydroxy methylpropanal (HMP)	3-hydroxy-2-methylpropanal
	3-hydroxy-2-methylpropanoic peroxy-nitrate (HMPPN)	3-hydroxy-2-methylpropanoic nitric peroxyanhydride
	isobutyraldehyde (ISOBUT)	isobutyraldehyde
	isobutyraldehyde peroxy-nitrate (ISOBPN)	isobutyric nitric peroxyanhydride
	tridecane	tridecane
	peroxyacetyl nitrate (PAN)	acetic nitric peroxyanhydride
	2-oxopropanoic peroxy-nitrate (2OPN)	nitric 2-oxopropanoic peroxyanhydride



1

2 **Figure S1:** Chromatograms of NO<sub>2</sub>, PAN, and MPAN in the NO<sub>2</sub>/APN analyser (retention times  
 3 10, 20, and 80 s, respectively). Top panel – signals from NO<sub>2</sub> and MPAN are observed when  
 4 introducing MPAN into the chamber due to a small decomposition yield of MPAN in room-  
 5 temperature Teflon lines. This decomposition is not observed in the headspace of pure MPAN in  
 6 tridecane when the standard is kept cold and the sampling line is short (< 0.3 m). Bottom panel –  
 7 photooxidation of MPAN over the course of 3 h, when the MPAN signal decreases and PAN is  
 8 observed to form. The NO<sub>2</sub> signal does not change significantly, possibly due to the  
 9 compensating effects of decreasing signal from MPAN and increasing signal from other sources.

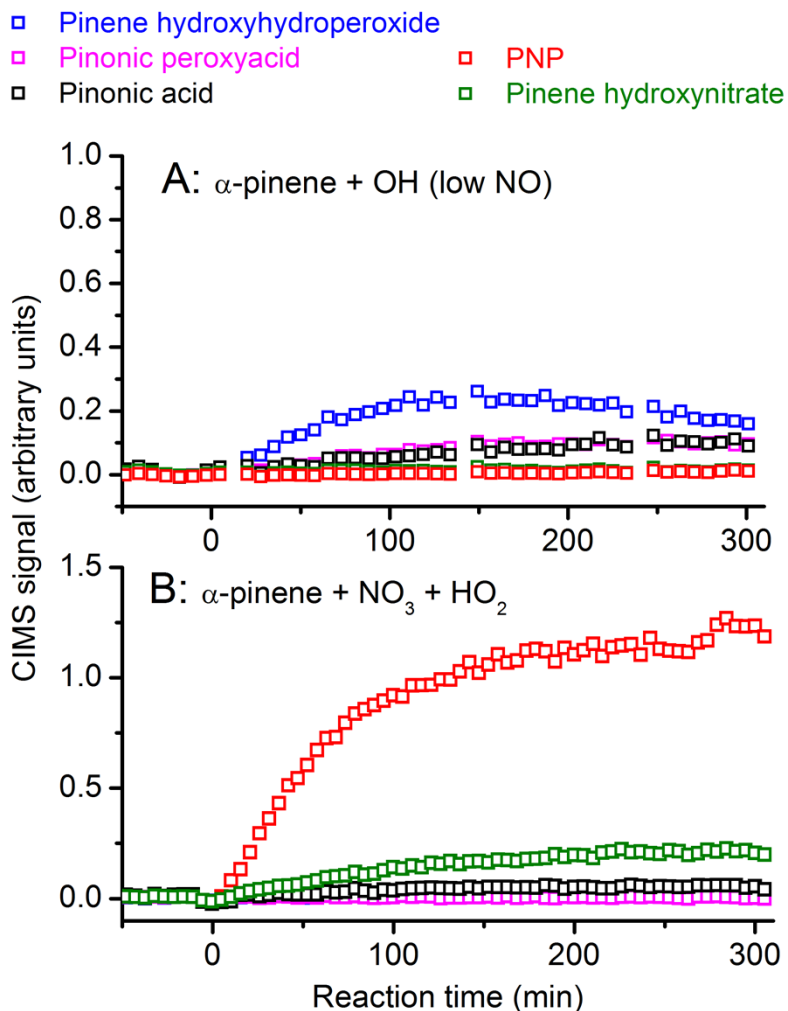
10



1

2 **Figure S2:** Characterization of 2-methylglyceric acid with A: proton NMR using DMSO  
 3 solvent, the semi-pure mixture (containing 7% acetonitrile) was further purified through  
 4 crystallization and B: tandem mass (MS/MS) with triple quadrupole CIMS, the 2-methylglyceric  
 5 acid is observed only as its fluoride transfer ion with  $\text{CF}_3\text{O}^-$  and collision-induced dissociation  
 6 leads primarily to the deprotonated compound ( $\text{C}_4\text{H}_7\text{O}_4^-$ ).

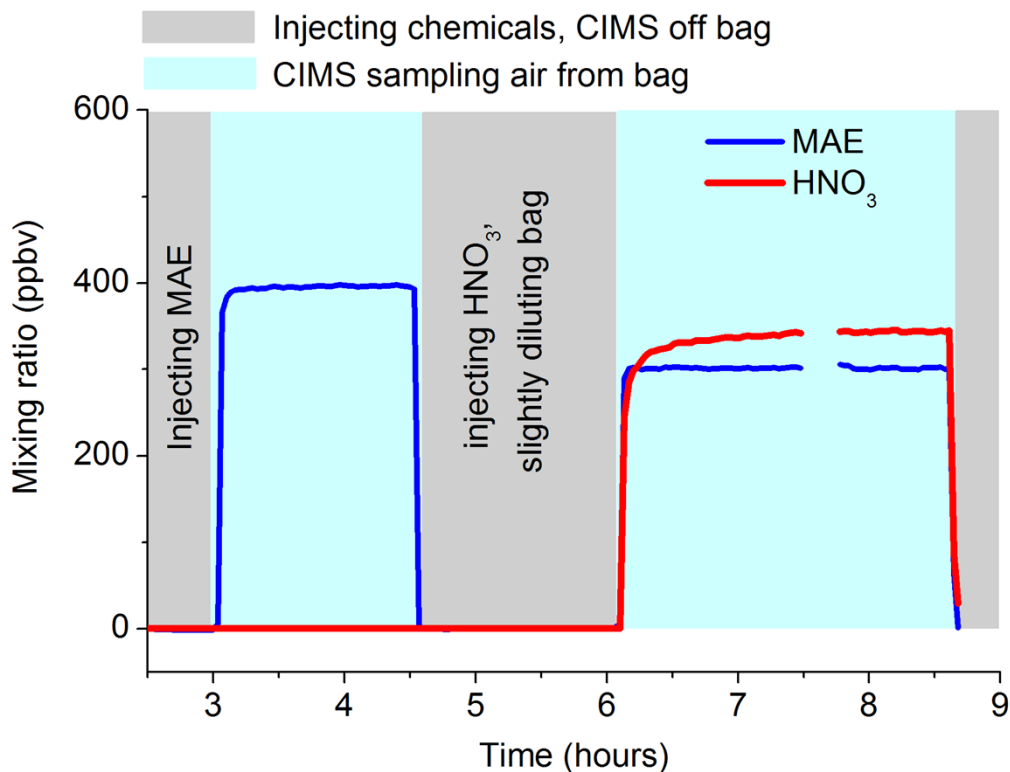
7



1

2 **Figure S3:** Ion intensity data (not converted to mixing ratio) from the negative ion mode CIMS  
 3 during control experiments performed with  $\alpha$ -pinene: (A) The pinene nitrooxyhydroperoxide  
 4 (PNP, red markers) used as a tracer for NO<sub>3</sub> in this work is not formed under the low-NO  
 5 conditions that were used to photooxidize MPAN; (B) PNP is only formed (and is a major  
 6 product) when NO<sub>3</sub> is available to oxidize  $\alpha$ -pinene (or  $\beta$ -pinene) in the presence of HO<sub>2</sub> radicals  
 7 (generated from photolysis of HCHO in these experiments). Pinonaldehyde (measured in  
 8 positive ion mode, not shown) is also a major product in both oxidation experiments.

9



1

2 **Figure S4:** Monitoring the loss of MAE to the walls of a 1000 L Teflon bag, filled with dry  
 3 purified ('zero') air (relative humidity < 5% in the bag). MAE did not demonstrate any  
 4 observable wall loss under these conditions. Injections of nitric acid (~ 500 ppbv injected, ~300  
 5 ppbv observed in the gas phase) did not change the wall loss behaviour of MAE over the course  
 6 of 2.5 hours, after which the instrument was taken off the bag.

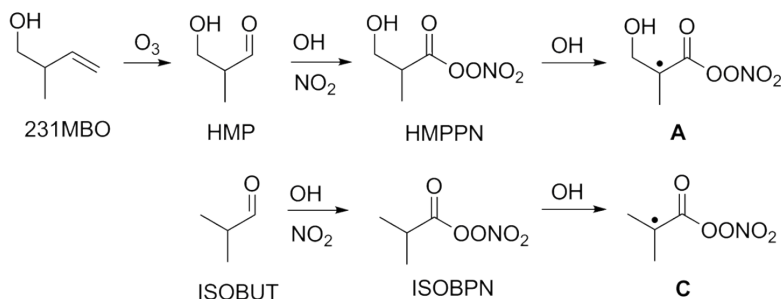
7

## 1 Section S1: Photooxidation of saturated analogues of MPAN

2 Lactone formation has been suggested only for APNs of aldehydes with a beta-alkenyl moiety,  
3 MACR and acrolein.<sup>1</sup> Here, we investigate the extent to which saturated APNs may access a  
4 similar reaction pathway. The OH-initiated oxidation of saturated and unsaturated compounds  
5 proceeds predominantly through abstraction and addition channels, respectively, illustrated here  
6 for ethylene and ethane:



9 The abstraction-generated alkyl radical is less energetic than the alkyl radical formed via  
10 addition of OH. It is unclear whether most of the abstraction radicals would be collisionally  
11 stabilized or if the  $-\text{C}(\text{O})\text{OONO}_2$  neighboring group enhances its decomposition. To investigate  
12 the effects of alkyl radical energetics, we conducted additional experiments using radicals **A** and  
13 **C** (Fig. 6) that are analogous to **A\***. The radical **A** (produced in Exp. #11) is the thermalized  
14 version of **A\***, given its formation mechanism; and **C** (produced in Exp. #10) is structurally  
15 similar to **A**, but missing the hydroxyl group. As the results of both experiments are consistent,  
16 we limit the discussion only to the chemistry of **A**, a third-generation oxidation intermediate of  
17 2-methyl-but-3-ene-1-ol (231MBO).



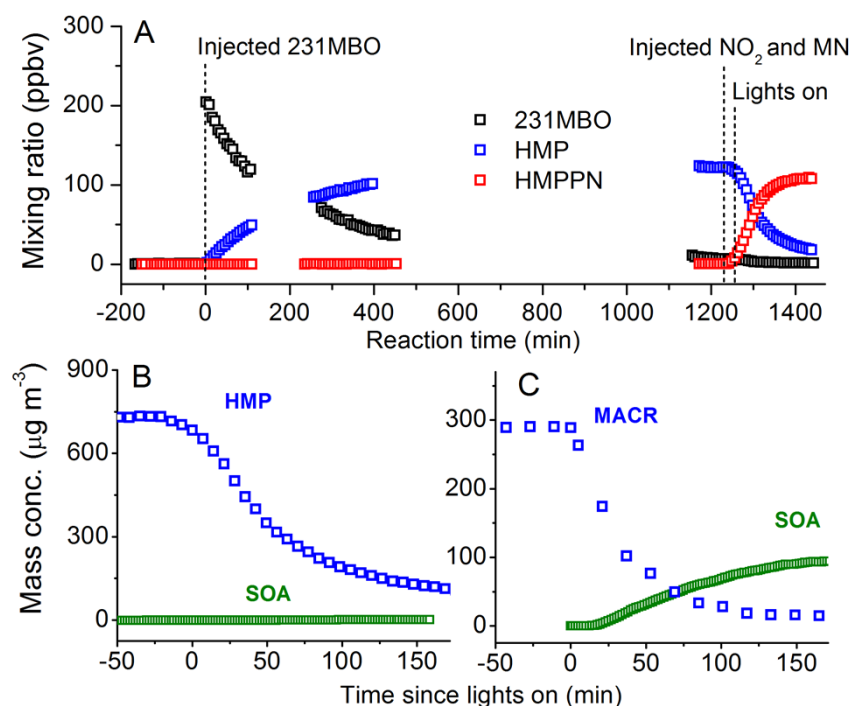
19 **Figure S5:** Gas-phase synthesis of beta alkyl radicals from saturated APNs:  
20 hydroxymethylpropanoyl peroxyxynitrate (HMPPN) and isobutanoyl peroxyxynitrate (ISOBPN).

21

22 Figure S6A shows the formation of the 3-hydroxy, 2-methylpropanoyl peroxyxynitrate (HMPPN)  
23 from a chamber experiment. HMPPN is the precursor of **A** from 231MBO, formed in a synthetic  
24 scheme that involves ~ 21 h of dark ozonolysis chemistry (to react away most of the C=C bonds  
25 of 231MBO) followed by a shorter phase of high- $\text{NO}_2$  photooxidation. Ozonolysis of 231MBO  
26 produces the aldehyde hydroxymethyl propanal (HMP) in high yield alongside the simplest  
27 Criegee ( $\text{CH}_2\text{OO}$ ), which is observed by CIMS as its bimolecular product with water,  
28 hydroxymethylhydroperoxide (not shown).<sup>2</sup> The ozonolysis period (performed without an OH  
29 scavenger) produced a small yield of SOA (< 3%) that has the same temporal behaviour as HMP.



1 After the stabilization of the dark gas-phase mixture, NO<sub>2</sub> and methyl nitrite were injected and  
 2 the near-UV lamps were switched on to initiate the OH-oxidation chemistry in the presence of  
 3 NO<sub>2</sub>. The slight decay of HMP prior to initiation of photochemistry (e.g., starting at - 20 min,  
 4 Fig. 7B) is due to reaction with NO<sub>3</sub>, formed after the injection of NO<sub>2</sub> through its reaction with  
 5 O<sub>3</sub>; however, this slower chemistry is promptly overtaken by the OH oxidation that occurred in  
 6 the photolytic period.



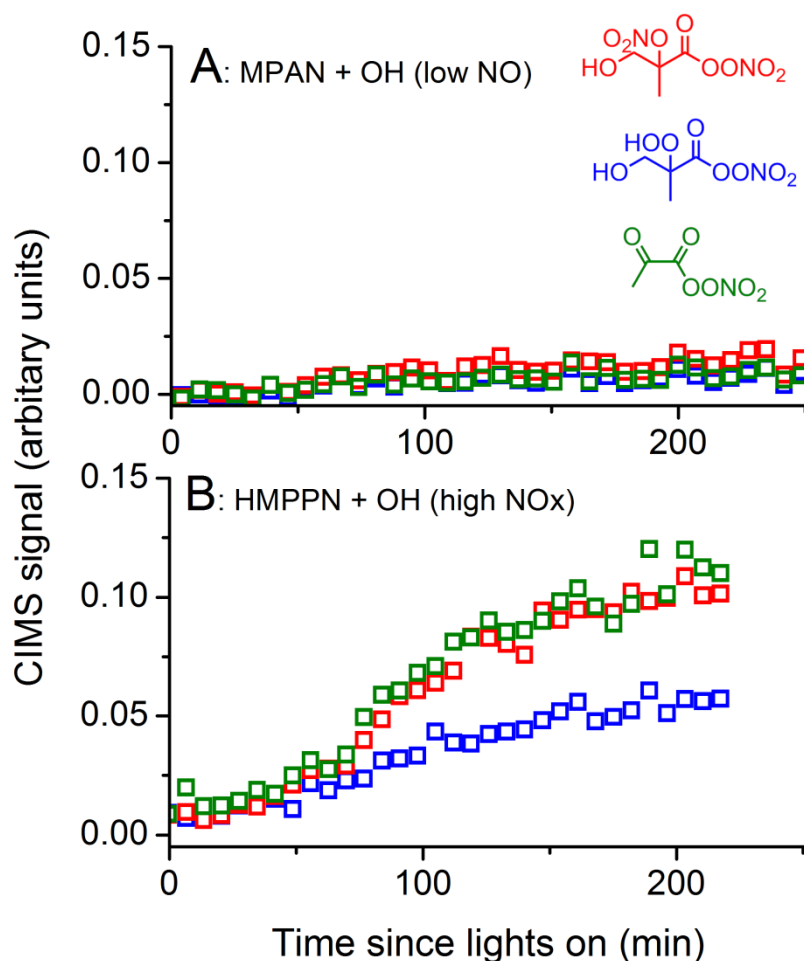
7

8 **Figure S6:** SOA formation from saturated vs. unsaturated APNs: (A) the results from Exp. #11  
 9 where 231MBO is ozonized into its aldehyde HMP, followed by high-NO<sub>2</sub> photooxidation to the  
 10 APN (HMPPN) with methyl nitrite (MN) as an OH precursor; (B) the reaction shown in panel A  
 11 where the time axis is renormalized to start when UV lights are switched on and SOA from the  
 12 dark period is subtracted; (C) similar to panel B but with MACR as the hydrocarbon (Exp. # 9).  
 13 Both vertical axes in panels B and C are with respect to mass. Breaks in data occur when  
 14 instruments are not sampling from the chamber.

15

16 The photochemistry of HMP (and that of HMPPN) does not produce additional SOA (Fig. S6B,  
 17 << 1 % SOA yield from HMP). In comparison, when MACR is oxidized in a similar manner  
 18 (Fig. S6C), SOA is observed to grow after a ~ 15 min delay. A delay in observing SOA is fairly  
 19 typical when seed particles are not used (Fig. 4) because the lower threshold for particle diameter  
 20 in this work is 20 nm. Additionally, the SOA should be second-generation so the observed delay  
 21 may encompass a chemical delay. As HMP and MACR both produce the APNs, which upon

1 oxidation form structurally identical alkyl radicals, the results suggest that the difference in  
 2 excess energy of **A** and **A\*** is responsible for the disparate SOA formation behaviour.



3

4 **Figure S7:** High-NO and low-NO compounds from alkylperoxyl (RO<sub>2</sub>) radical **B:** the  
 5 hydroxynitrates (RO<sub>2</sub>+NO → RONO<sub>2</sub>, red), hydroxyhydroperoxides (RO<sub>2</sub>+HO<sub>2</sub> → ROOH + O<sub>2</sub>,  
 6 blue), and 2-oxopropanoyl peroxyxynitrate (2OPN, green) from (A) the MPAN photooxidation and  
 7 (B) the HMPPN photooxidation. The production of HAC from MPAN (reaching ~0.25 at the 250  
 8 min mark) and HMPPN (reaching 1.8 at the 220 min mark), via different mechanisms, is greater  
 9 than the production of the shown compounds.

10

11 Experimental evidence for HMPPN reaction and **A** + O<sub>2</sub> reaction can be provided by the  
 12 CIMS observations of alkylperoxyl radical (RO<sub>2</sub>) and alkoxy radical (RO) reaction products  
 13 (Fig. S7, see Fig. 6 in the main text for the mechanism). During the photolytic period, we  
 14 observed the minor products of the RO<sub>2</sub> + NO reaction channel, the hydroxynitrates (RO<sub>2</sub> + NO  
 15 → RONO<sub>2</sub>) and the major product of the RO<sub>2</sub> + HO<sub>2</sub> reaction channel, the

1 hydroxyhydroperoxides ( $\text{RO}_2 + \text{HO}_2 \rightarrow \text{ROOH} + \text{O}_2$ ) from the HMPPN + OH reaction. These  
2 radical termination products have low volatility (e.g., the hydroperoxide has a molecular formula  
3 of  $\text{C}_4\text{H}_7\text{NO}_8$ ) in addition to low yields, resulting in low analyte signals in the CIMS. We also  
4 observed the major products from the high-NO reaction ( $\text{RO}_2 + \text{NO} \rightarrow \text{RO} + \text{NO}_2 \rightarrow$   
5 decomposition products), which include HAC (~ 25% from HMP) and the APN of  
6 pyruvaldehyde (2-oxopropanoyl peroxyxynitrate (2OPN), < 1% from HMP, green trace in Fig.  
7 S7).<sup>3</sup> The relative yields of HAC is 3 – 30 times higher compared to the 2OPN when estimated  
8 from HMPPN; however the absolute yields are not available as the amount of HMPPN reacted is  
9 unknown. The disparity in relative yields may be due to the expected propensity for 2OPN to  
10 decompose (via the  $\text{NO}_2$  and  $\text{NO}_3$  channels)<sup>3</sup> compared to the high stability of HAC. The  
11 formation of  $\text{RO}_2$  radical termination products and RO decomposition products in the MPAN +  
12 OH reaction was negligible (Fig. S7a). The HAC formation in the MPAN + OH reaction is via  
13 HMML decomposition. Together with SOA data and HMPPN-derived product observations, the  
14  $\text{RO}_2$  reaction products provides a consistent picture of predominantly HMML formation from  
15 MPAN + OH and  $\text{RO}_2$  formation from HMPPN + OH.

16

17

18

## 19 References

- 20 1. H. G. Kjaergaard, H. C. Knap, K. B. Ørnsø, S. Jørgensen, J. D. Crouse, F. Paulot and P. O.  
21 Wennberg, *J. Phys. Chem. A*, 2012, 116, 5763-5768.  
22 2. P. Neeb, F. Sauer, O. Horie and G. K. Moortgat, *Atmos. Environ.*, 1997, 31, 1417-1423.  
23 3. J. J. Orlando, G. S. Tyndall, S. B. Bertman, W. Chen and J. B. Burkholder, *Atmos. Environ.*,  
24 2002, 36, 1895-1900.

25